

RESEARCH ARTICLE

Open Access

Evolutionary diversification and characterization of the eubacterial gene family encoding DXR type II, an alternative isoprenoid biosynthetic enzyme

Lorenzo Carretero-Paulet^{1,2*}, Agnieszka Lipska¹, Jordi Pérez-Gil³, Félix J Sangari⁴, Victor A Albert¹ and Manuel Rodríguez-Concepción^{3*}

Abstract

Background: Isoprenoids constitute a vast family of natural compounds performing diverse and essential functions in all domains of life. In most eubacteria, isoprenoids are synthesized through the methylerythritol 4-phosphate (MEP) pathway. The production of MEP is usually catalyzed by deoxyxylulose 5-phosphate reductoisomerase (DXR-I) but a few organisms use an alternative DXR-like enzyme (DXR-II).

Results: Searches through 1498 bacterial complete proteomes detected 130 sequences with similarity to DXR-II. Phylogenetic analysis identified three well-resolved clades: the DXR-II family (clustering 53 sequences including eleven experimentally verified as functional enzymes able to produce MEP), and two previously uncharacterized NAD(P)-dependent oxidoreductase families (designated DLO1 and DLO2 for DXR-II-like oxidoreductases 1 and 2). Our analyses identified amino acid changes critical for the acquisition of DXR-II biochemical function through type-I functional divergence, two of them mapping onto key residues for DXR-II activity. DXR-II showed a markedly discontinuous distribution, which was verified at several levels: taxonomic (being predominantly found in Alphaproteobacteria and Firmicutes), metabolic (being mostly found in bacteria with complete functional MEP pathways with or without DXR-I), and phenotypic (as no biological/phenotypic property was found to be preferentially distributed among DXR-II-containing strains, apart from pathogenicity in animals). By performing a thorough comparative sequence analysis of GC content, 3:1 dinucleotide frequencies, codon usage and codon adaptation indexes (CAI) between DXR-II sequences and their corresponding genomes, we examined the role of horizontal gene transfer (HGT), as opposed to an scenario of massive gene loss, in the evolutionary origin and diversification of the DXR-II subfamily in bacteria.

Conclusions: Our analyses support a single origin of the DXR-II family through functional divergence, in which constitutes an exceptional model of acquisition and maintenance of redundant gene functions between non-homologous genes as a result of convergent evolution. Subsequently, although old episodic events of HGT could not be excluded, the results supported a prevalent role of gene loss in explaining the distribution of DXR-II in specific pathogenic eubacteria. Our results highlight the importance of the functional characterization of evolutionary shortcuts in isoprenoid biosynthesis for screening specific antibacterial drugs and for regulating the production of isoprenoids of human interest.

Keywords: DXR-II, Isoprenoid metabolism, Horizontal gene transfer, Gene loss, Functional divergence

* Correspondence: lorenzoc@buffalo.edu; manuel.rodriguez@cragenomica.es

¹Institute for Plant Molecular and Cell Biology - IBMCP (CSIC-UPV), Integrative Systems Biology Group, C/ Ingeniero Fausto Elio s/n., Valencia 46022, Spain

³Centre for Research in Agricultural Genomics (CRAG), CSIC-IRTA-UAB-UB, Campus UAB, Bellaterra, Barcelona 08193, Spain

Full list of author information is available at the end of the article

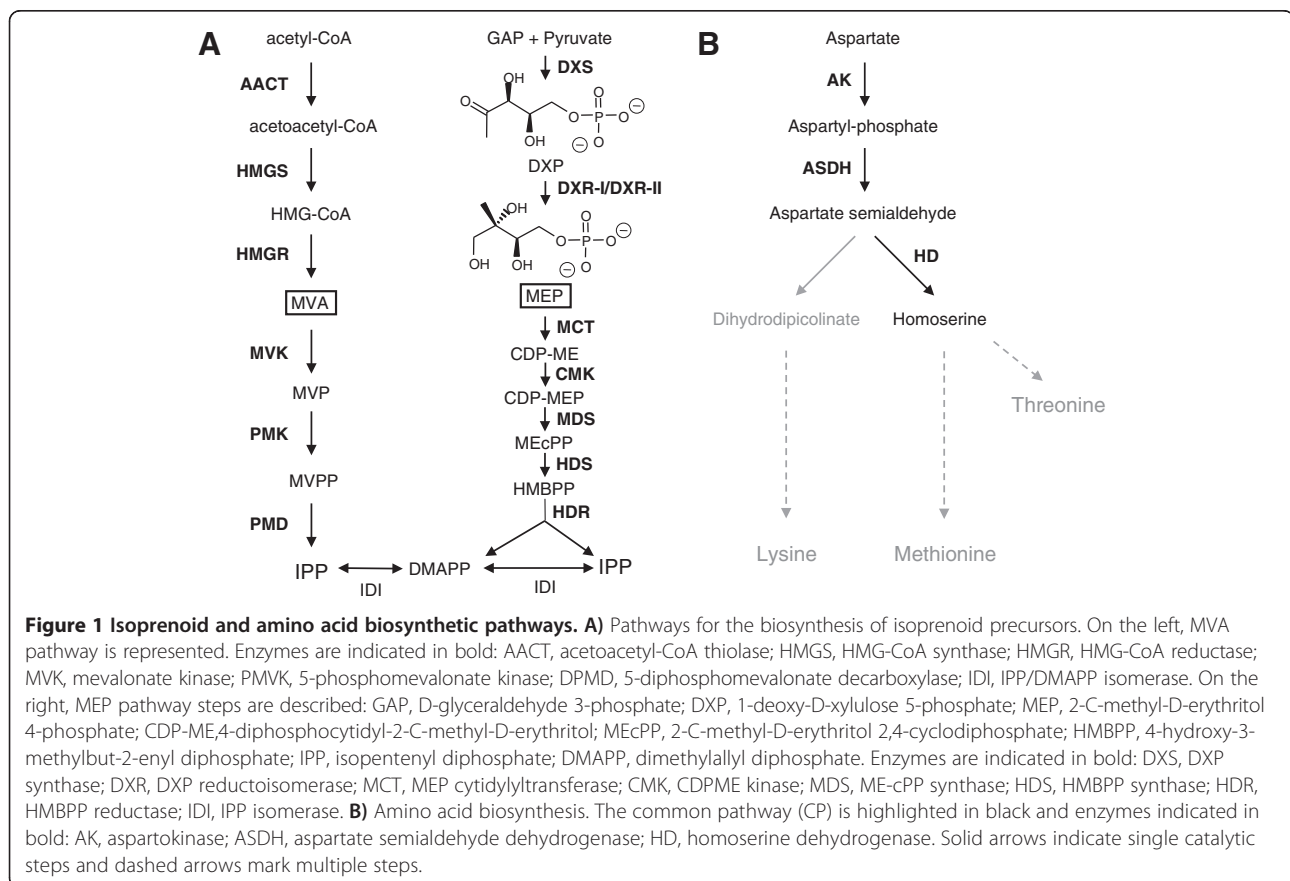
Background

Isoprenoids constitute the largest family of natural compounds both at a structural and functional level [1-3]. They are found in all the three domains of life (bacteria, archaea, and eukaryotes). Despite their diversity in structures and functions, all isoprenoids derive from the common five-carbon precursors isopentenyl diphosphate (IPP) and its isomer dimethylallyl diphosphate (DMAPP). IPP can be synthesized through two independent metabolic pathways, the mevalonate (MVA) pathway, or the more recently elucidated methylerythritol 4-phosphate (MEP) pathway [4] (Figure 1). In most eubacteria, isoprenoids are synthesized through the MEP pathway, while a few species use the MVA pathway, both pathways, or none, the latter obtaining their isoprenoids from host cells [5-8]. Previous analysis suggested that eukaryotes have inherited MEP and MVA pathways genes from eubacteria and archaeobacteria, respectively, as reflected by their phylogenetic distribution [5]. In plants, plastidial IPP and DMAPP are synthesized through the MEP pathway, whereas cytosolic and mitochondrial isoprenoids are synthesized through the MVA pathway [4,9]. Non-photosynthetic simpler plastid-bearing organisms, such as the apicomplexan protists, solely use the MEP pathway [10]. In contrast, in yeast and animals, all isoprenoids are synthesized through the

MVA pathway [11]. The lack of MEP pathway enzymes in non-plastid bearing eukaryotes suggests that these genes were acquired through gene transfer to the nucleus from the eubacterial endosymbiotic ancestors that gave rise to plastids [5,12].

Isoprenoids are essential in all eubacteria in which they have been studied, playing key roles in several core cellular functions e.g. ubiquinones and menaquinones, which act as electron carriers of the aerobic and anaerobic respiratory chains respectively, and dolichols, which are required for cell wall peptidoglycan synthesis [13]. Because of the essential role of the MEP pathway in most eubacteria and its absence from animals, it has been proposed as a promising new target for the development of novel antibiotics [14,15]. Besides that, many isoprenoids also have substantial industrial, pharmacological, and nutritional interest [16]. Therefore, understanding the biochemical and genetic plasticity of isoprenoid biosynthesis in bacteria is crucial to attempt its pharmacological block or to be used in biofactories for the production of isoprenoids of human interest.

The occurrence of alternative enzymes for isoprenoid biosynthesis in specific bacterial lineages has been previously reported [17]. The enzyme 3-hydroxy-3-methylglutaryl-CoA reductase (HMGR), which catalyzes the



rate-limiting step of the MVA pathway, is structurally distant from its archaeobacterial and eukaryotic homologs in most eubacteria [8,18,19]. Similarly, two different classes of isopentenyl diphosphate isomerase (IDI), the enzyme catalyzing the isomerization of IPP to produce DMAPP, have been identified in bacteria: type I IDI (similar to its animal, fungi and plant counterparts) and type II IDI, acquired from archaeobacteria and apparently unrelated to the latter [20-22]. Although IDI activity is only essential in organisms dependent on the MVA pathway for IPP and isoprenoid biosynthesis, both types of IDI have been identified in bacterial strains dependent on the MEP pathway [7].

We recently reported the occurrence of a group of bacteria harbouring the entire set of enzymes of the MEP pathway with the exception of 1-deoxy-d-xylulose 5-phosphate (DXP) reductoisomerase (DXR), the enzyme catalyzing the NADPH-dependent production of MEP from DXP in the first committed step of the pathway. In these species, a novel family of previously uncharacterized oxidoreductases related to homoserine dehydrogenases (HD) involved in the common pathway (CP) of amino acid biosynthesis (Figure 1), was found to perform the DXR biochemical reaction [23]. This alternative enzyme, referred to as DXR-like (DRL) or DXR type II (DXR-II) to distinguish it from the canonical DXR (renamed DXR-I), displayed a markedly discontinuous distribution. DXR-II was found forming single or multigene families in bacterial strains from diverse taxonomic groups, independent of the presence or absence of a DXR-I sequence in their genome [23].

Different evolutionary scenarios might explain DXR-II emergence and evolutionary diversification. In this study we examined how the DXR-II family emerged through functional divergence from related oxidoreductase families and identified amino acid changes critical for the acquisition of its specific biochemical function. Furthermore, we assess the contrasting roles of horizontal gene transfer (HGT) and massive gene loss, major forces in microbial genome evolution known to affect other genes involved in IPP and isoprenoid biosynthesis [24], in the discontinuous distribution of DXR-II across eubacteria.

Results

DXR-IIs cluster into a single clade closely related to two uncharacterized oxidoreductase families

The complete proteomes of 1489 eubacterial strains were screened for the occurrence of DXR-II sequences using the protein sequence from *Brucella melitensis* biovar *abortus* 2308 DXR-II (formerly *Brucella abortus* 2308, gene id: 83269188) as a query [23]. To reduce false positives caused by hits corresponding to distantly related sequences, we applied a best reciprocal hit

criterion i.e. orthology was assumed only if two genes in each different genome are each other's best hit [25]. Indeed, eight sequences were not confirmed as reciprocal best hits, including two identified in a previous survey conducted following a unidirectional BLAST search approach [23], and these were consequently discarded from further analyses. 128 sequence hits were identified in as many bacterial strains (Table 1), belonging to a wide variety of the main bacterial taxonomic groups (Figure 2). Among these, two bacterial strains (*Mesorhizobium loti* MAFF303099 and *Ochrobactrum anthropi* ATCC 49188) had been previously shown to code for additional functional DXR-II paralogs [23] that were not identified by our analysis, specifically designed to identify co-orthologs in genome wide scans, but were added to the final dataset (Table 1).

Using the amino acid sequence alignment of the resulting full dataset of 130 hits (Additional file 1), a maximum likelihood (ML) phylogenetic analysis was performed (Figure 2 and Additional file 2). Alternative methods of phylogenetic inference (Bayesian -Additional file 3- and neighbor joining -Additional file 4) were also implemented, resulting in trees with almost identical topologies (unpublished data). Three main clades were consistently retrieved with high support values (Figure 2). A clade grouping 53 sequences, including 11 encoding for functional DXR-II as shown in complementation assays in [23] and Additional file 5, was designated as the DXR-II family and likely corresponds to actual DXR-II sequences (Figure 2). The remaining 77 sequences cluster into two additional clades and might not be true functional DXR-II sequences (Figure 2). As such, these were tentatively designated DLO1 and DLO2, for DXR-II-Like 1 and 2 Oxidoreductases. Indeed, four representative sequences belonging to the DLO1 and 2 families had also been previously tested for DXR-II activity, failing to complement the DXR defective mutant (Figure 2) [23].

DXR-II and DLO sequences showed similarity to NAD (P)-dependent oxidoreductases, and particularly to HD enzymes, at a sequence [23] and structural level [26]. Correspondingly, searches for INTERPRO functional domains identified the NAD-binding domain with a core Rossmann-type fold at the N-terminal region of every single protein sequence (domain 1; Figure 2). Up to five additional domains could also be found in DXR-II and DLO proteins. To examine whether these protein domains were differentially distributed across the DXR-II, DLO1, and DLO2 families, we mapped the architecture of protein domains onto the corresponding tree (Figure 2). Most sequences from the DXR-II family shared NAD-binding (domain 1) and SAF (domain 6) domains, while a significant fraction also included N-terminal NAD/NADP-binding domains of aspartate/homoserine dehydrogenase (domain 2). However, no common domain architecture

Table 1 List of DXR-II and DLO related sequences examined in this study

	Bacterial strain	UID	GenBank and RefSeq		Bacterial strain	UID	GenBank and RefSeq
DXR-II	<i>Anaerococcus prevotii</i> DSM 20548	59219	gi 257066990 ref YP_003153246.1	DLO1	<i>Frankia sp. Eul1c</i>	42615	gi 312199021 ref YP_004019082.1
	<i>Bacillus clausii</i> KSM-K16	58237	gi 56965002 ref YP_176733.1		<i>Gloeobacter violaceus</i> PCC 7421	58011	gi 37521773 ref NP_925150.1
	<i>Bacillus halodurans</i> C-125	57791	gi 15613337 ref NP_241640.1		<i>Hirschia baltica</i> ATCC 49814	59365	gi 254294497 ref YP_003060520.1
	<i>Bacillus pumilus</i> SAFR-032	59017	gi 157692210 ref YP_001486672.1		<i>Kineococcus</i> <i>radiotolerans</i> SRS30216	58067	gi 152964541 ref YP_001360325.1
	<i>Bartonella bacilliformis</i> KC583	58533	gi 121601844 ref YP_989368.1		<i>Methanospaerula</i> <i>palustris</i> E1-9c	59193	gi 219852978 ref YP_002467410.1
	<i>Bartonella clarridgeiae</i> 73	62131	gi 319898668 ref YP_004158761.1		<i>Nakamurella</i> <i>multipartita</i> DSM 44233	59221	gi 258653356 ref YP_003202512.1
	<i>Bartonella grahamii</i> <i>as4aup</i>	59405	gi 240851045 ref YP_002972445.1		<i>Nostoc azollae</i> 0708	49725	gi 298491811 ref YP_003721988.1
	<i>Bartonella henselae</i> str. Houston-1	57745	gi 49475991 ref YP_034032.1		<i>Nostoc punctiforme</i> PCC 73102	57767	gi 186681545 ref YP_001864741.1
	<i>Bartonella quintana</i> str. Toulouse	57635	gi 49474558 ref YP_032600.1		<i>Nostoc sp.</i> PCC 7120	57803	gi 17230323 ref NP_486871.1
	<i>Bartonella tribocorum</i> CIP 105476	59129	gi 163868831 ref YP_001610057.1		<i>Pseudomonas stutzeri</i> A1501	58641	gi 146282531 ref YP_001172684.1
	<i>Brucella abortus</i> bv. 1 str. 9-941	58019	gi 62317206 ref YP_223059.1		<i>Pseudomonas stutzeri</i> ATCC 17588 = LMG 11199	68749	gi 339494143 ref YP_004714436.1
	<i>Brucella abortus</i> S19	58873	gi 189022468 ref YP_001932209.1		<i>Pseudoxanthomonas</i> <i>spadix</i> BD-a59	75113	gi 357416048 ref YP_004929068.1
	<i>Brucella canis</i> ATCC 23365	59009	gi 161621022 ref YP_001594908.1		<i>Ramlibacter</i> <i>tataouinensis</i> TTB310	68279	gi 337280130 ref YP_004619602.1
	<i>Brucella melitensis</i> ATCC 23457	59241	gi 225686729 ref YP_002734701.1		<i>Rhodobacter</i> <i>sphaeroides</i> 2.4.1	57653	gi 77463590 ref YP_353094.1
	<i>Brucella melitensis</i> biovar Abortus 2308	62937	gi 83269188 ref YP_418479.1		<i>Rhodobacter</i> <i>sphaeroides</i> ATCC 17025	58451	gi 146278215 ref YP_001168374.1
	<i>Brucella melitensis</i> bv. 1 str. 16 M	57735	gi 17988671 ref NP_541304.1		<i>Rhodobacter</i> <i>sphaeroides</i> ATCC 17029	58449	gi 126462422 ref YP_001043536.1
	<i>Brucella microti</i> CCM 4915	59319	gi 256015731 ref YP_003105740.1		<i>Rhodobacter</i> <i>sphaeroides</i> KD131	59277	gi 221639432 ref YP_002525694.1
	<i>Brucella ovis</i> ATCC 25840	58113	gi 148558391 ref YP_001257886.1		<i>Rhodothermus marinus</i> DSM 4252	41729	gi 268316714 ref YP_003290433.1
	<i>Brucella pinnipedialis</i> B2/94	71131	gi 340792737 ref YP_004758201.1		<i>Rhodothermus marinus</i> SG0.5JP17-172	72767	gi 345303494 ref YP_004825396.1
	<i>Brucella suis</i> 1330	57927	gi 23500696 ref NP_700136.1		<i>Sphingomonas</i> <i>wittichii</i> RW1	58691	gi 148557435 ref YP_001265017.1

Table 1 List of DXR-II and DLO related sequences examined in this study (Continued)

<i>Brucella suis</i> ATCC 23445	59015	gij 163845083 ref YP_001622738.1		<i>Streptomyces griseus</i> subsp. <i>griseus</i> NBRC 13350	58983	gij 182439707 ref YP_001827426.1
<i>Chelativorans</i> sp. BNC1	58069	gij 110636013 ref YP_676221.1		<i>Xanthomonas campestris</i> pv. <i>campestris</i> str. 8004	57595	gij 77761197 ref YP_243248.2
<i>Chloroflexus aurantiacus</i> J-10-fl	57657	gij 163846900 ref YP_001634944.1		<i>Xanthomonas campestris</i> pv. <i>campestris</i> str. ATCC 33913	57887	gij 77747863 ref NP_637377.2
<i>Chloroflexus</i> sp. Y-400-fl	59085	gij 222524722 ref YP_002569193.1		<i>Xanthomonas campestris</i> pv. <i>campestris</i> str. B100	61643	gij 188991706 ref YP_001903716.1
<i>Clostridium difficile</i> 630	57679	gij 126700028 ref YP_001088925.1	DLO2	<i>Achromobacter xylosoxidans</i> A8	59899	gij 311109080 ref YP_003981933.1
<i>Clostridium difficile</i> CD196	41017	gij 260683992 ref YP_003215277.1		<i>Acidiphilium cryptum</i> JF-5	58447	gij 148260557 ref YP_001234684.1
<i>Clostridium difficile</i> R20291	40921	gij 260687652 ref YP_003218786.1		<i>Acidiphilium multivorum</i>	63345	gij 326403752 ref YP_004283834.1
<i>Eubacterium limosum</i> KIST612	59777	gij 310828050 ref YP_003960407.1		<i>Acidovorax ebreus</i> TPSY	59233	gij 222110742 ref YP_002553006.1
<i>Finegoldia magna</i> ATCC 29328	58867	gij 169824217 ref YP_001691828.1		<i>Acidovorax</i> sp. JS42	58427	gij 121594656 ref YP_986552.1
<i>Halanaerobium hydrogeniformans</i>	60191	gij 312144614 ref YP_003996060.1		<i>Actinosynnema mirum</i> DSM 43827	58951	gij 25637798 ref YP_003101458.1
<i>Listeria innocua</i> Clip11262	61567	gij 16799625 ref NP_469893.1		<i>Agrobacterium</i> sp. H13-3	63403	gij 332715931 ref YP_004443397.1
<i>Listeria ivanovii</i>	73473	gij 347547952 ref YP_004854280.1		<i>Agrobacterium tumefaciens</i> str. C58	57865	gij 15891768 ref NP_357440.1
<i>Listeria monocytogenes</i>	43671	gij 284800826 ref YP_003412691.1		<i>Anaeromyxobacter</i> sp. Fw109-5	58755	gij 153005951 ref YP_001380276.1
<i>Listeria monocytogenes</i> 08-5923	43727	gij 284994012 ref YP_003415780.1		<i>Arthrobacter</i> sp. FB24	58141	gij 116672147 ref YP_833080.1
<i>Listeria monocytogenes</i> EGD-e	61583	gij 16802589 ref NP_464074.1		<i>Azorhizobium caulinodans</i> ORS 571	58905	gij 158423518 ref YP_001524810.1
<i>Listeria monocytogenes</i> HCC23	59203	gij 217965360 ref YP_002351038.1		<i>Bordetella avium</i> 197 N	61563	gij 187476836 ref YP_784860.1
<i>Listeria monocytogenes</i> serotype 4b str. CLIP 80459	59317	gij 226223175 ref YP_002757282.1		<i>Bordetella bronchiseptica</i> RB50	57613	gij 33599421 ref NP_886981.1
<i>Listeria monocytogenes</i> serotype 4b str. F2365	57689	gij 46906791 ref YP_013180.1		<i>Bordetella parapertussis</i> 12822	57615	gij 33595139 ref NP_882782.1

Table 1 List of DXR-II and DLO related sequences examined in this study (Continued)

	<i>Listeria welshimeri</i> serovar 6b str. SLCC5334	61605	gij116871936 ref YP_848717.1	<i>Bordetella petrii</i> DSM 12804	61631	gij163858833 ref YP_001633131.1
	<i>Mesorhizobium ciceri</i> biovar biserrulae WSM1271	62101	gij319781195 ref YP_004140671.1	<i>Bradyrhizobium</i> japonicum USDA 110	57599	gij27382926 ref NP_774455.1
	<i>Mesorhizobium loti</i> MAFF303099 (1)	57601	gij13473132 ref NP_104699.1	<i>Bradyrhizobium</i> sp. BTA1	58505	gij148252763 ref YP_001237348.1
	<i>Mesorhizobium loti</i> MAFF303099 (2)	57601	gij13475431 ref NP_106995.1	<i>Bradyrhizobium</i> sp. ORS278	58941	gij146343223 ref YP_001208271.1
	<i>Mesorhizobium</i> <i>opportunatum</i> WSM2075	40861	gij337266026 ref YP_004610081.1	<i>Candidatus Pelagibacter</i> ubique HTCC1062	58401	gij71083552 ref YP_266271.1
	<i>Ochrobactrum anthropi</i> ATCC 49188 (1)	58921	gij153008718 ref YP_001369933.1	<i>Cupriavidus necator</i> N-1	68689	gij339328796 ref YP_004688488.1
	<i>Ochrobactrum anthropi</i> ATCC 49188 (2)	58921	gij153011435 ref YP_001372649.1	<i>Cupriavidus taiwanensis</i>	61615	gij194292943 ref YP_002008850.1
	<i>Pelagibacterium</i> halotolerans B2	74393	gij357386128 ref YP_004900852.1	<i>Methylidium</i> petroleiphilum PM1	58085	gij124268433 ref YP_001022437.1
	<i>Roseobacter litoralis</i> Och 149	54719	gij339504759 ref YP_004692179.1	<i>Methylobacterium</i> nodulans ORS 2060	59023	gij220926646 ref YP_002501948.1
	<i>Sebaldeella termitidis</i> ATCC 33386	41865	gij269122365 ref YP_003310542.1	<i>Methylobacterium</i> radiotolerans JCM 2831	58845	gij170751253 ref YP_001757513.1
	<i>Sinorhizobium fredii</i> NGR234	59081	gij227820170 ref YP_002824141.1	<i>Methylobacterium</i> sp. 4-46	58843	gij170738904 ref YP_001767559.1
	<i>Starkeya novella</i> DSM 506	48815	gij298294348 ref YP_003696287.1	<i>Mycobacterium</i> smegmatis str. MC2 155	57701	gij118472915 ref YP_885297.1
	<i>Tepidanaerobacter</i> sp. Re1	66873	gij332798945 ref YP_004460444.1	<i>Nocardioopsis</i> dassonvillei subsp. dassonvillei DSM 43111	49483	gij297561288 ref YP_003680262.1
	<i>Thermosediminibacter</i> oceani DSM 16646	51421	gij302389988 ref YP_003825809.1	<i>Paracoccus denitrificans</i> PD1222	58187	gij119386102 ref YP_917157.1
	<i>Verminephrobacter</i> eiseniae EF01-2	58675	gij121609190 ref YP_996997.1	<i>Polaromonas</i> sp. JS666	58207	gij91787595 ref YP_548547.1
DLO1	<i>Anabaena variabilis</i> ATCC 29413	58043	gij75907337 ref YP_321633.1	<i>Polymorphum gilvum</i> SL003B-26A1	65447	gij328544682 ref YP_004304791.1
	<i>Chloroflexus aggregans</i> DSM 9485	58621	gij219849032 ref YP_002463465.1	<i>Polynucleobacter</i> necessarius subsp. asymbioticus QLW- P1DMWA-1	58611	gij145589731 ref YP_001156328.1
	<i>Coraliomargarita</i> akajimensis DSM 45221	47079	gij294053940 ref YP_003547598.1	<i>Pusillimonas</i> sp. T7-7	66391	gij332284324 ref YP_004416235.1

Table 1 List of DXR-II and DLO related sequences examined in this study (Continued)

<i>Coxiella burnetii</i> CbuG_Q212	58893	gij 212211864 ref YP_002302800.1	<i>Rhodopseudomonas</i> <i>palustris</i> BisB5	58441	gij 91978550 ref YP_571209.1
<i>Coxiella burnetii</i> CbuK_Q154	58895	gij 212217809 ref YP_002304596.1	<i>Rhodospirillum rubrum</i> ATCC 11170	57655	gij 83594471 ref YP_428223.1
<i>Coxiella burnetii</i> Dugway 5 J108-111	58629	gij 154707185 ref YP_001423500.1	<i>Spirochaeta</i> <i>smaragdinae</i> DSM 11293	51369	gij 302337774 ref YP_003802980.1
<i>Coxiella burnetii</i> RSA 331	58637	gij 161830312 ref YP_001597660.1	<i>Spirochaeta</i> sp. Buddy	63633	gij 325972507 ref YP_004248698.1
<i>Coxiella burnetii</i> RSA 493	57631	gij 29655123 ref NP_820815.1	<i>Streptomyces</i> <i>flavogriseus</i> ATCC 33331	40839	gij 357414986 ref YP_004926722.1
<i>Cyanotheca</i> sp. PCC 7425	59435	gij 220910534 ref YP_002485845.1	<i>Streptomyces</i> sp. <i>SirexA</i> AcpoE	72627	gij 345003166 ref YP_004806020.1
<i>Cyclobacterium</i> <i>marinum</i> DSM 745	71485	gij 343084038 ref YP_004773333.1	<i>Variovorax paradoxus</i> EPS	62107	gij 319794630 ref YP_004156270.1
<i>Deinococcus</i> <i>maricopensis</i> DSM 21211	62225	gij 320332781 ref YP_004169492.1	<i>Variovorax paradoxus</i> S110	59437	gij 239816446 ref YP_002945356.1
<i>Desulfococcus</i> <i>oleovorans</i> Hxd3	58777	gij 158521221 ref YP_001529091.1	<i>Xanthobacter</i> <i>autotrophicus</i> Py2	58453	gij 154244830 ref YP_001415788.1

UID (taxonomy) Unique IDentifier.

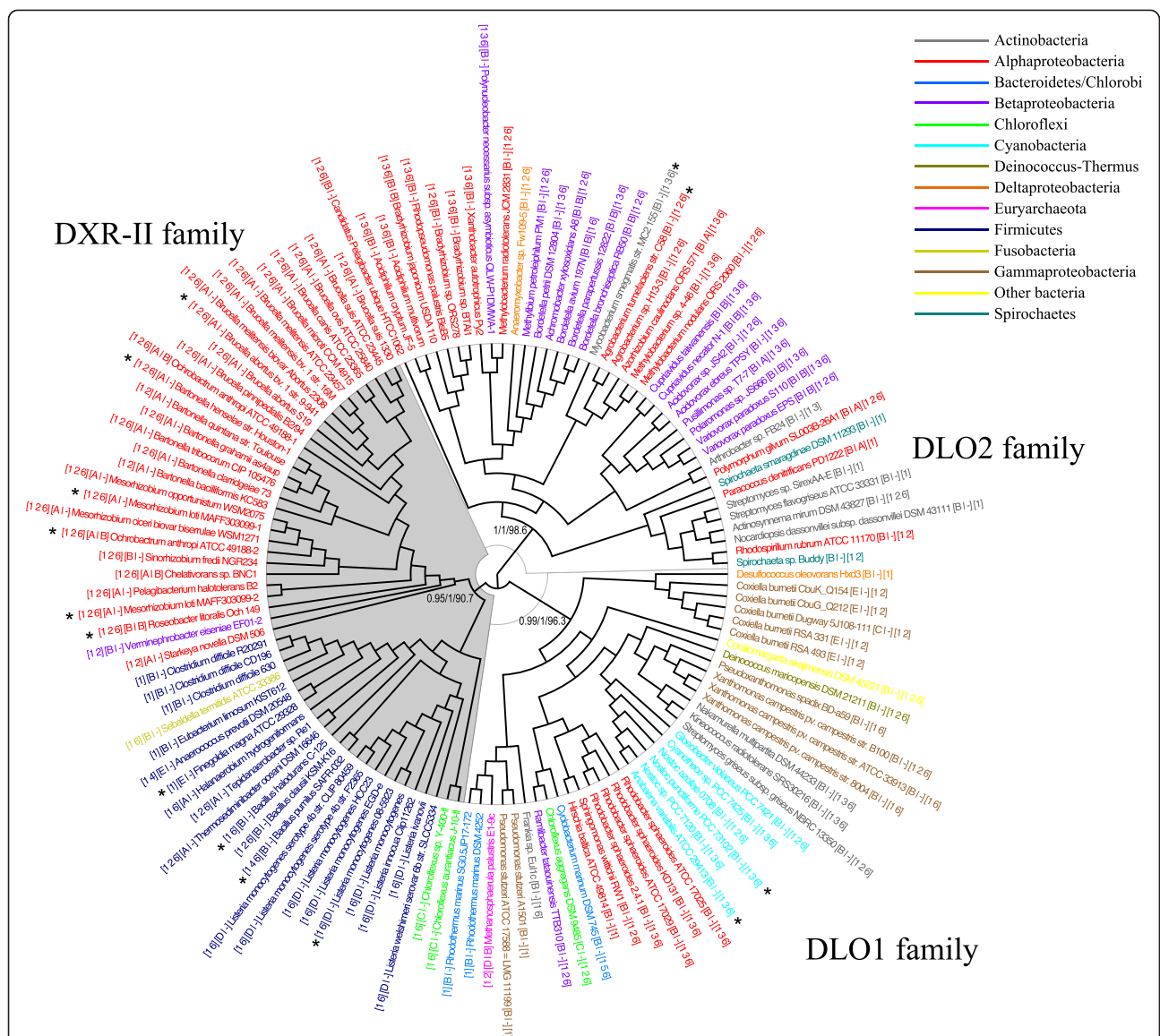


Figure 2 Phylogeny of DXR-II and DLO related sequences. ML cladogram depicting the evolutionary relationships among 53 DXR-II and 77 related protein sequences. Three clades defining main families are indicated. Statistical support on relevant clades is indicated by values next to nodes (ML aLRT support values/BA posterior probabilities/NJ bootstrap values). Sequence names are colored according to taxonomical groups (see legend). Sequence names include the bacterial strain name, followed by two pairs of square brackets: the first pair encloses the classification of the given bacterial strain according to the distribution of enzymes of the i) MEP and MVA pathways, left side of the vertical bar (i.e. classes A, +MEP pathway enzymes -DXR; B, +MEP pathway enzymes +DXR; C, -MEP + MVA pathway enzymes -DXR; D, +MEP + MVA pathway enzymes +DXR; E, -MEP -MVA pathway enzymes -DXR) and ii) CP pathway, right side of the vertical bar (i.e. A, complete CP pathway; B, incomplete CP pathway -AK_HD). The second pair of brackets represents the INTERPRO protein functional domains found i.e. 1, NAD(P)-binding domain (IPR016040); 2, Aspartate/homoserine dehydrogenase, NAD-binding (IPR005106); 3, Oxidoreductase, N-terminal (IPR000683); 4, Dihydrodipicolinate reductase, N-terminal (IPR000846); 5, Quinate/shikimate 5-dehydrogenase/glutamyl-tRNA reductase (IPR006151); 6, SAF domain (IPR013974). Asterisks indicate sequences for which DXR-II activity was previously tested through complementation assays [23] and Additional file 5.

was shared among proteins within families DLO1 and DLO2.

The DXR-II family emerged through functional divergence
 Phylogenetic analysis revealed the shared ancestry of all functional DXR-II, supporting their common evolutionary

origin, and suggested the functional divergence of this family from related oxidoreductases through the acquisition of DXR-II specific biochemical activity. To examine the role of specific amino acid substitutions in functional specialization of DXR-II protein sequences, two different statistical approaches under a ML framework were followed. The first one permits the detection of

amino acid sites subjected to different evolutionary rates between families under examination, i.e., highly conserved in a family but variable in the other (type-I functional divergence) [27]. The second approach relies on site-specific shifts of amino acid physicochemical properties in positions otherwise highly conserved in each family (type-II functional divergence) [28].

Given the ML tree topology (Figure 2), the ML estimates of the theta (θ) coefficients for type-I functional divergence between the DXR-II family and families DLO1 and DLO2 were statistically significant in both cases (Table 2). This implies that structural and/or functional selective constraints at some sites have shifted significantly after the divergence of DXR-II from both DLO families. In contrast, the corresponding tests did not support type-II functional divergence (Table 2). Moreover, 28 and 34 specific amino acid residues, including 8 and 11 with high posterior probabilities, were predicted as responsible for type-I functional divergence of DXR-II from DLO families 1 and 2, respectively (Table 2). Interestingly, seven sites detected as key for functional divergence were shared in analyses between the DXR-II family and both the DLO1 and DLO2 families.

These sites were mapped onto the corresponding amino acid sequence alignment (Additional file 1 and Additional file 6: Table S1). At many of these sites, amino acid residues are highly conserved in DXR-II sequences, but are variable in the DLO1 (e.g. positions 161 and 429 in *B. melitensis biovar abortus 2308* DXR-II), the DLO2 (e.g. positions 210, 248 and 324), or both the DLO1 and the DLO2 (e.g. positions 35, 64, 118, 121, 122, 133, 197, 229, 250, 291, 320, 330, 346, 351, 353, 413, 428, 429, 432) families, likely reflecting a change in their functional roles. Some apparently represented minor changes, as they involved amino acids with similar physicochemical features (e.g. positions 291 or 428). Some others involved radical amino acid changes, such as position 121, occupied by the highly conserved Gly in DXR-II proteins, but also by the unrelated Ala and Ser amino acids in DLO1 and DLO2 proteins. Another example is position 229, filled by the absolutely conserved polar amino acid Thr in DXR-II proteins, but replaced by the highly hydrophobic Leu, Ile and Val amino acids in DLO1 or the physicochemically unrelated Pro, Ser and Ala residues in DLO2. Likewise, position 250, with a basic polar His found in all but four DXR-II proteins was replaced by different hydrophobic amino acids, and finally position 351, with a conserved Val in most DXR-II proteins was substituted by different physicochemically unrelated amino acids in DLO1 and DLO2 proteins.

To gain further insights into their putative functional impact, the amino acid changes detected as related to functional divergence of DXR-II were mapped onto the

three-dimensional structure of *B. melitensis biovar abortus 2308* DXR-II in its apo form and in complex with the competitive inhibitor fosmidomycin (Figure 3) [26]. Predicted sites were mostly distributed through the middle catalytic domain, but some were also found in the COOH-terminal and NH₂-terminal NADP-binding domains (Figure 3A). Two predicted sites corresponded to the conserved residues 229 and 320, identified as important for DXR-II activity [26]. Thr229, together with Lys191 and Lys193, serve to anchor fosmidomycin, presumably participating in the proper binding of the substrate (Figure 3B). Arg320 is located in a cavity at the dimer interface and, together with positions Glu174, Phe178 and Tyr322, may be involved in interactions between the two subunits of the DXR-II dimer (Figure 3C).

DXR-IIs show a discontinuous taxonomic, metabolic and phenotypic distribution among eubacteria

The markedly scattered distribution of sequences belonging to the DXR-II family across higher order eubacterial taxonomic groups was previously observed [23]. In this up-to-date survey, DXR-IIs were found as encoded by the genomes of free-living eubacteria strains mostly from Alphaproteobacteria (26 strains, mainly from the genera *Brucella*, 11, and *Bartonella*, 6) and Firmicutes (21 strains, mainly from the genus *Listeria*, 9). However, genes coding for functional DXR-II representatives were also found in the genomes of three additional distantly related bacterial taxonomic lineages i.e. the Chloroflexi, Betaproteobacteria and Fusobacteria (Figure 2). Within the DXR-II family, Alphaproteobacteria, Firmicutes and Chloroflexi sequences clustered into separate subclades, while the single Betaproteobacteria and Fusobacteria representatives grouped within the Alphaproteobacteria and Firmicutes subclades, respectively (Figure 2).

We examined the distribution of functional DXR-II at lower taxonomical levels. For example, the occurrence of discontinuities was evident when we mapped DXR-II onto a tree depicting the evolutionary relationships of 72 alphaproteobacterial species (Additional file 7) [30]. *DXR-II* genes could only be found in the genomes of 25 strains among the 64 with fully sequenced genomes represented in the tree. They mainly belong to the order Rhizobiales, although significant hits were also retrieved from other taxonomic ranks, such as Rhodospirillales or Rhodobacteraceae. Within these alphaproteobacterial groups, strains whose genomes contained genes both encoding and not encoding DXR-II and/or DXR-I could be found. Discontinuities in DXR-II distribution could be appreciated with, e.g., the closely related pairs of Rhodospirillales species *Magnetospirillum magneticum* AMB-1/*Rhodospirillum rubrum* ATCC 11170 and *Acidiphilium cryptum* JF-5/*Gluconobacter oxydans* 621H. More strikingly, we have retrieved a DXR-II

Table 2 Analysis of functional divergence

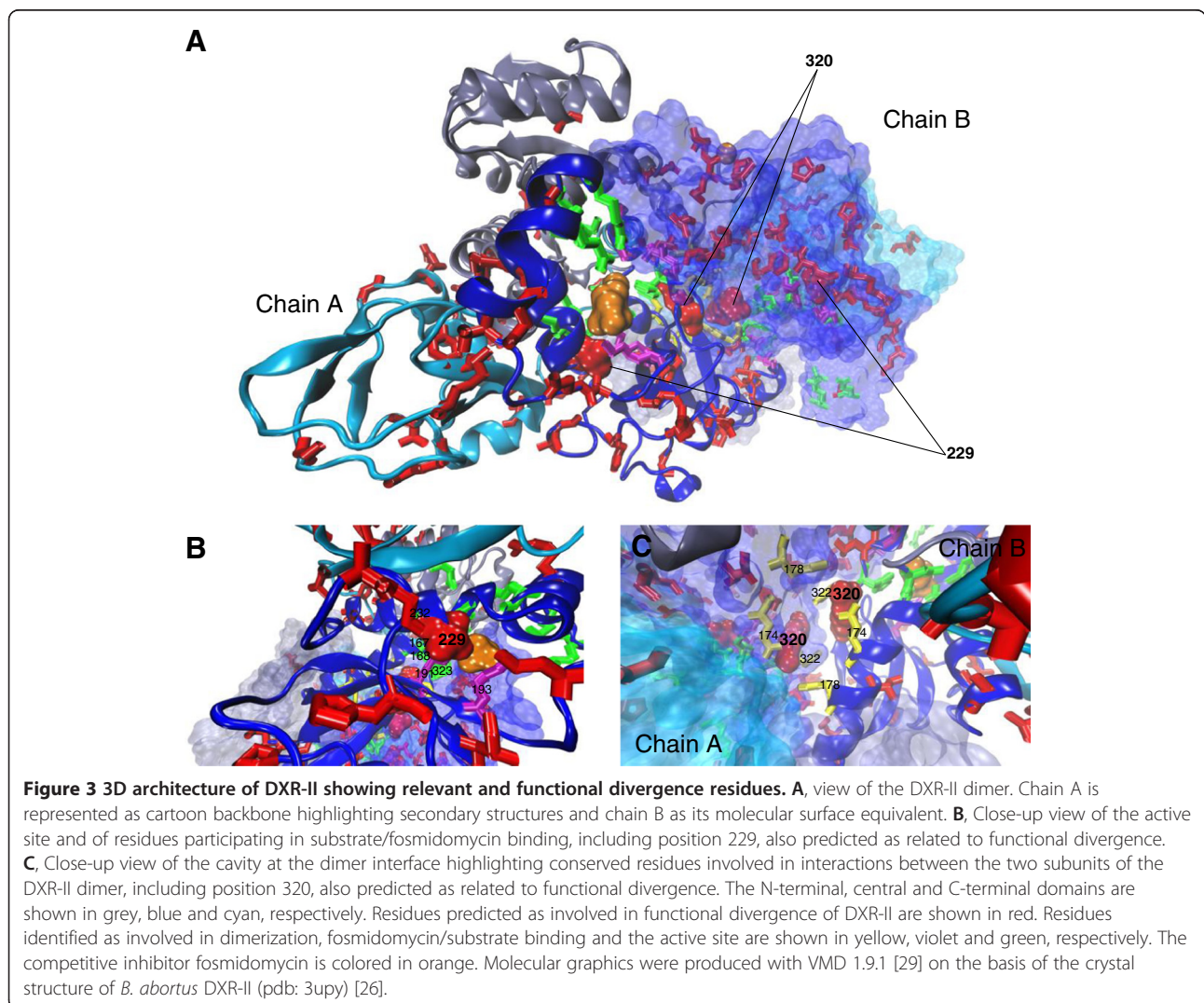
Functional divergence	Families	Coefficient $\theta \pm SE$	Critical amino acid sites ($Q_k > 0.7$; *, $Q_k > 0.95$)
Type I	DXR-II vs DLO1	$\theta_1 = 0.277 \pm 0.045$ (LRT = 83.233; $p = 7.292E-20$)	35 , 46, 118, 121, 146, 161*, 176, 198*, 205* , 218, 229, 234, 237, 247*, 265, 282* , 291 , 297, 310 , 340, 342, 351* , 353*, 376, 404*, 410 , 422, 424, 429
	DXR-II vs DLO2	$\theta_1 = 0.253 \pm 0.043$ (LRT = 114.991; $p = 7.907E-27$)	35 , 47, 64, 122*, 128, 133, 197*, 202, 205 , 210, 239, 248, 250*, 253*, 258*, 260, 282 , 291 , 296, 305, 310* , 311*, 314, 320, 324*, 330*, 346, 351* , 359, 383*, 410* , 413, 428*, 432
Type II	DXR-II vs DLO1	$\theta_2 = -0.998 \pm 0.487$	
	DXR-II vs DLO2	$\theta_2 = -1.115 \pm 0.575$	

p = posterior probability values; SE Standard Error. LRT and resulting p -values are shown in parentheses. Critical amino acid sites detected as related to functional divergence with $Q_k > 70\%$ (*, $Q_k > 95\%$) are listed. Seven sites predicted as related to functional divergence of DXR-II from both families DLO1 and DLO2 are indicated in bold. Numbering refers to *Brucella melitensis* biovar abortus 2308 DXR-II protein sequence.

sequence only in one out of the five examined genomes of strains from *Rhodopseudomonas palustris* (strain BisB5), a feature perhaps related to the metabolic versatility attributed to this species [31] (Additional file 7). A similar patchy distribution of DXR-II was observed

when DXR-II and DXR-I were mapped onto a phylogeny of Firmicutes (Additional file 8) [32].

Searches for enzymes of the MEP and MVA pathways of IPP and isoprenoid biosynthesis were also performed (Additional file 6: Table S2). The 51 DXR-II-containing



eubacterial strains were classified according to the distribution of enzymes of these pathways, revealing the occurrence of multiple patterns (Figure 2 and Additional file 6: Table S3). The majority of surveyed eubacterial genomes contained genes coding for enzymes of the MEP pathway, but a significant number of them had lost one or more of these enzymes. DXR-I would have been preferentially lost among Alphaproteobacterial strains, but some losses were also found in Firmicutes and Chloroflexi (class A). These species would then exclusively rely on DXR-II for IPP biosynthesis through the MEP pathway. A group, mainly composed of Firmicutes strains showed genes encoding both DXR-II and DXR-I (class B). A significant number of genomes also encoded for enzymes of the MVA pathway. Some of these strains would then use solely the MVA pathway for isoprenoid biosynthesis, such as the two Chloroflexi representatives (class C). DXR-II activity has been experimentally shown from one of these strains, *Chloroflexus auranticus* J-10-fl, by complementation assays (Additional file 5). Most of them also have a complete and functional MEP pathway, such as *Listeria monocytogenes* (class D) [6]. Finally, in the genomes of two Firmicutes strains (*Anaerococcus prevotii* DSM 20548 and *Finegoldia magna* ATCC 29328) no genes encoding enzymes from the MEP (apart from DXR-II) or the MVA pathways could be found (class E). Interestingly however, DXR-II activity had been confirmed experimentally for the latter [23].

Similarly, the distribution of DXR-II was compared to that of enzymes of the CP pathway of amino acid biosynthesis. The CP represents three enzymatic steps. The first is the phosphorylation of aspartate, carried out by AK leading to β -aspartyl-phosphate, which in turn is oxidized by an ASDH to aspartate semialdehyde. Subsequently, HD catalyses the reduction of aspartate beta-semialdehyde into homoserine, in the third and last step of the CP pathway (Figure 1). The evolutionary diversification of enzymes of the CP in bacteria is known to have been shaped by gene duplication and fusion events, resulting in bifunctional AK_HD proteins [33]. Most genomes of the 51 DXR-II-containing strains encoded AK and HD. The genomes of five strains also showed bifunctional AK_HD genes, while the genomes of only three Alphaproteobacteria strains encoded for ASDH and were believed to have functional CP (class B) (Figure 1 and Additional file 6: Table S3). However, none of the genomes of DXR-II-containing strains encoded the complete set of enzymes of the CP (class A, AK, HD, AK_HD and ASDH).

We next examined the distribution of biological properties across DXR-II-containing bacterial strains. For this purpose, we projected the data contained in the NCBI's Microbial Organism Information Page onto the original set of 1489 bacterial strains, after correcting for

ambiguities and redundancies. The database, available for download at ftp://ftp.ncbi.nlm.nih.gov/genomes/genomeprj_archive/, included categories related to the ecological requirements of the organism (e.g. habitat, oxygen requirement, salinity, temperature range, optimal temperature), morphological features (e.g., shape, arrangement, endospores and motility) and additional phenotypic traits (e.g., Gram stain, dinucleotide GC content, genome size and pathogenicity). The distribution of properties across DXR-II- and non DXR-II-containing eubacterial strains is shown in Table 3. To test whether any of these biological properties were differentially represented in the subset of 51 eubacterial strains containing DXR-II regarding the remaining non-DXR-II harbouring strains, we performed Fishers' exact tests. According to these tests, none of the categories related to the ecological requirements of the organism showed a biased representation among DXR-II-containing strains, suggesting that these organisms may not live in shared habitats. A similar unbiased pattern of distribution was found for additional morphological and phenotypic features (Table 3). Only the category "pathogenic in animals" showed a significant overrepresentation among DXR-II-containing strains (Table 3). Similarly, for quantitative properties, such as genome size, GC content and optimal growth temperature, a Student's T test was performed to assess significance of the differences between means. Again, none of the tests were significant (Table 3).

Comparative sequence-based analysis of HGT in DXR-II evolution

The markedly discontinuous phylogenetic distribution shown by DXR-II might be explained by recurrent events of HGT occurring between unrelated bacterial strains. So long as the DXR-II sequence retains sequence features of the donor strain significantly distinct from that of the genome of the recipient strain, they could be inferred as being acquired by HGT. Consequently, comparative nucleotide sequences analyses of DXR-II against their host genomes could yield clues about their origin and the putative role of HGT in the distribution of DXR-II across eubacteria.

Several methods and criteria were applied to identify signatures of HGT (please see Methods for a complete description). Firstly, GC content at the three codon positions, as well as the total, was estimated. As previously observed [34,35], GC content was relatively constant among genes of a particular species' genomes, although displaying wide variation among species (Additional file 6: Table S4). This was particularly evident at the third codon position, as the majority of these sites are synonymous and, consequently, differences due to mutational biases are higher. In contrast, the first and second codon positions appear to be more conserved between genomes and

Table 3 Distribution of biological properties in DXR-II and non-DXR-II containing bacterial strains and statistical tests of enrichment

Biological properties	Number of strains		p-value
	DXR-II	Non-DXR-II	
Habitat	41	1166	
Host-associated	18	383	0.36
Multiple	16	330	0.33
Specialized	3	148	ND
Terrestrial	2	94	ND
Aquatic	2	211	ND
Oxygen Req	39	1137	
Facultative	15	404	0.76
Aerobic	15	413	0.88
Anaerobic	9	284	ND
Salinity	7	245	
Non-halophilic	6	171	ND
Moderate halophilic	1	30	ND
Temp. range	38	1202	
Mesophilic	36	1013	0.64
Thermophilic	2	107	ND
Optimal temp. ^a	38.61 (18)	41.21 (555)	0.27
Genome Size ^a	3.73 (48)	3.59 (1456)	0.50
GC Content ^a	48.23 (45)	48.63 (1193)	0.84
Shape	43	1239	
Rod	29	794	0.90
Coccobacillus	6	21	ND
Coccus	5	188	ND
Filament	2	20	ND
Short rod	1	2	ND
Arrangement	35	899	
Singles	17	501	0.77
Pairs	9	209	ND
Chains	4	107	ND
Groups	3	3	ND
Filaments	2	22	ND
Endospores	18	626	
Yes	6	121	ND
No	12	505	0.71
Motility	27	947	
Yes	22	579	0.37
No	5	365	ND
Gram Stain	39	1050	
-	22	704	0.60
+	17	344	0.35

Table 3 Distribution of biological properties in DXR-II and non-DXR-II containing bacterial strains and statistical tests of enrichment (Continued)

Pathogenic in	DXR-II	Non-DXR-II	p-value
Animal	15	181	0.04
Human	14	264	0.50
No	13	521	0.11

P-values resulting from Fisher's exact tests are shown for categories represented in at least 10 bacterial strains. Test significant at $p < 0.05$ is shown in bold type. ^a, for these quantitative properties, the average value (number of strains is shown between parentheses) and p-values resulting from Student's T tests performed to assess significance of the differences between means are shown.

are, consequently, less informative (Additional file 6: Table S4). The GC contents of all DXR-II coding sequences were compared to the mean for all genes encoded by the corresponding genomes. DXR-II from both Chloroflexi representatives and the single Fusobacteria representative *Sebaldella termitidis* ATCC 33386 showed significantly lower GCt and GC3 content regarding the respective mean for all genes in the genome (Additional file 6: Table S4). A fourth bacterial strain, *Rhizobium* NGR234, showed higher GCt and GC3 content (Additional file 6: Table S4).

Secondly, we examined for biases in dinucleotide relative frequencies, a remarkably stable property of the DNA of an organism claimed to constitute a 'genomic signature' that can discriminate sequences from different organisms [36]. We focused on the dinucleotide biases at third and first (3:1) codon positions, which are less sensitive to selective constraints [37]. Consequently, the 3:1 dinucleotide frequencies were calculated for all DXR-II coding sequences and for the entire set of genes in the corresponding genomes. They both showed significant variation across organisms, and therefore could be used as such genomic signatures. Significance of the differences between DXR-II genes and their genomes were examined by calculating the dinucleotide relative abundance difference or σ difference (Additional file 6: Table S5) [36]. Pairwise co-variation was further assessed through the Spearman and Kendall rank tests (Additional file 6: Table S5). In all but one example, both Spearman's ρ and Kendall's τ correlation coefficients indicated strong positive correlation. An exception was provided by *Halanaerobium hydrogeniformans*, which showed negative correlation. All tests revealed significant covariation of 3:1 dinucleotide frequencies of DXR-II with the frequencies of the corresponding genomes, contrary to the expectations of HGT.

Next, we estimated relative synonymous codon usages (RSCU) values, which provide with a simple effective measure of synonymous codon usage bias. Differences in RSCU between DXR-II genes and all other genes in each corresponding genome were assessed by means of χ^2

tests (Additional file 6: Table S6) [34]. Chloroflexi strains and *S. termitidis* ATCC 33386 showed the higher χ^2 statistic values, revealing higher variation. However, none of the tests was significant, indicating that *DXR-II* genes have a codon usage patterns consistent with that of their corresponding genomes, and therefore unlikely to reflect HGT.

Finally, we examined the degree of bias in codon usage of *DXR-II* genes towards the codon usage of the most expressed genes by comparing Codon Adaptation Index (CAI) values. A significant deviation from the average CAI of the genome was found in strains of Chloroflexi and *S. termitidis* ATCC 33386 (Additional file 6: Table S7).

Discussion and conclusions

The structural and functional diversity of isoprenoids correlates with the existence of a wide biochemical and genetic plasticity for their biosynthesis [17]. In eubacteria, this is commonly achieved through the use of alternative metabolic pathways and enzymatic steps in specific lineages. Interesting examples are provided by HMGR and IDI, which are encoded by at least two distinct gene families in bacteria. In this paper we focus in *DXR-II*, recently characterized as an alternative family to *DXR-I* in performing the second step of the MEP pathway of isoprenoid biosynthesis in a selected group of eubacteria [23].

Apart from the NAD-binding domain with a core Rossmann-type fold found at the N-terminal region of all oxidoreductases, no significant similarity at the sequence level was observed between *DXR-I* and *DXR-II* to infer homology [23]. Correspondingly, the recent determination of the *DXR-II* crystal structure showed only slight structural relationship with *DXR-I* proteins and revealed a unique arrangement of the active site [26]. Examples of enzymes catalyzing identical reactions through the same catalytic mechanisms but showing structurally unrelated active sites are known outside the isoprenoid field [38-41]. In some of these though, key catalytic residues may be conserved between functionally redundant enzymes, as also reported for *DXR-I* and *DXR-II* [26]. *DXR-I* and *DXR-II* likely represent analogous genes that evolved redundant biochemical functions through mechanistic convergence.

Our results support the emergence of the *DXR-II* family through type I, but not type II, functional divergence from DLO1 and DLO2 families of previously uncharacterized oxidoreductases. These data suggest that *DXR-II* acquired additional structural and/or functional constraints rather than shifted constraints in amino acids that were already ancestrally constrained. Amino acid changes critical for functional divergence and acquisition of *DXR-II* biochemical activity were predicted, many of them corresponding to positions highly conserved in

DXR-II, but otherwise variable in DLO1 and/or DLO2. Interestingly, two of these predicted amino acids, Thr229 and Arg320, had been previously identified for their role in fosmidomycin/substrate binding and in dimerization, respectively [26], suggesting that functional shifts in a limited number of amino acid positions could be at the origin of the acquisition of *DXR-II* biochemical activity.

It could be assumed that the MEP pathway is the ancestral route for IPP and isoprenoid biosynthesis in eubacteria, including the membrane-associated hopanoids, which are among the oldest known biomolecules [42]. The entire set of genes encoding for enzymes involved in the MEP pathway, including *DXR-I*, has been found widespread in all eubacterial taxonomic groups [5]. In a significant number of *DXR-II*-containing eubacterial genomes (31), including those from closely related strains, *DXR-I* has been lost. This raises the question of how *DXR-II* evolved in *DXR-I* containing strains, as acquisition of redundant biochemical activities should not be favoured by evolution. The *DXR-II* family could have emerged under an ecological context that conferred a selective advantage to the emergence and maintenance of a functionally redundant enzyme, e.g. when gene dosage is selectively advantageous. Due to the wide and diverse functions played by isoprenoids and their essential role for cell viability, critical situations in which their biosynthesis was absolutely required may have occurred multiple times throughout eubacterial evolution. Emergence of the *DXR-II* family should have occurred at an early time in evolution, as supported by the scattered distribution of *DXR-II* and related oxidoreductases from DLO1 and DLO2 families in distantly related lineages of eubacteria. After relaxation of that burst in selective constraints for isoprenoid biosynthesis, some strains could then have lost one redundant enzyme, commonly *DXR-II*, which shows less catalytic activity in vitro [26]. In addition, maintenance of *DXR-II*, which shows less sensitivity to inhibition by fosmidomycin than *DXR-I* [26], might have provided a selective advantage in bacterial strains sharing the same ecological niches as those naturally producing the antibiotic (e.g. *Streptomyces* species [43]).

The taxonomic distribution of *DXR-II* across eubacteria showed a marked discontinuity, which was also verified at the metabolic and phenotypic level. Although most genes encoding *DXR-II* were found in eubacteria with the MEP pathway, their occurrence was not linked to a unique pattern of distribution of enzymes of the MEP or MVA pathways. Similarly, HD, the oxidoreductase family that showed the highest level of similarity with *DXR-II*, was found in most *DXR-II*-containing bacterial strains, but not all. In addition, examination of the distribution of biological properties across *DXR-II*-containing

strains showed maintenance of DXR-II in the genomes was not linked to a unique pattern of ecological or phenotypic traits. The only exception was 'pathogenic in animals,' significantly enriched among DXR-II-containing strains, reflecting the occurrence of DXR-II among pathogenic strains of *Brucella*, *Bartonella*, *Listeria* and *Clostridium* [44-47].

The outstanding phylogenetic discontinuity in DXR-II distribution across eubacteria could be explained through two alternative, though not mutually exclusive, evolutionary mechanisms, i.e., gene gain through HGT or gene loss. HGT is known to have shaped the evolution of multiple metabolic pathways, including IPP and isoprenoid biosynthesis [8,24,48]. However, a unique event of HGT cannot properly explain DXR-II phylogeny. According to our phylogenetic analysis, such HGT events should instead have occurred at different time points throughout eubacterial evolution, e.g. between the Alphaproteobacteria and Firmicutes phyla, between the Alphaproteobacteria and Betaproteobacteria classes within the proteobacteria phylum, between Firmicutes and specific Chloroflexi strains or between Firmicutes and specific Fusobacteria. More recently, HGT should also have occurred between closely related Alphaproteobacteria or Firmicute strains. If this was the case, HGT events should have left a signature of atypical sequence features in *DXR-II* genes, provided they were recent enough and occurring between distantly taxonomically related donor and acceptor bacterial strains [34,35]. Weak signatures of HGT were found only in Chloroflexi and the Fusobacterium *S. termitidis* ATCC 33386 at the level of GC content and CAI values. However, no biases in dinucleotide frequencies or codon usage were observed in any strain comparison. These results suggested that HGT events were not at the origin of all discontinuities, or were so ancient that *DXR-II* genes ameliorated their sequence to specific base composition and codon usage of the host genome, making them indistinguishable from ancestral sequences [34,35].

Consequently, although old episodic events of HGT cannot be excluded, the alternative hypothesis of recurrent *DXR-II* (or eventually *DXR-I*) gene loss is more likely to explain DXR-II phylogeny. This mechanism has been traditionally considered less parsimonious, as it involves a complex ancestor and gene loss events occurring independently at multiple evolutionary lineages. However, recent works suggests that, on average, gene loss might be a more likely event than gene gain through HGT [49-51].

The DXR-I/DXR-II model constitutes an exceptional natural model to experimentally test the emergence and maintenance of redundant gene function between non-homologous genes as a result of convergent evolution, as opposed to their emergence from intragenomic duplicates,

or paralogs. Furthermore, our results highlight the importance of the functional characterization of evolutionary shortcuts in isoprenoid biosynthesis for screening specific antibacterial drugs and for regulating the production of isoprenoids of human interest.

Methods

Sequence and phylogenetic analysis

Sequence databases from the whole sequenced genomes of 1489 bacterial strains were downloaded from the NCBI. Orthologs of enzymes from the MEP and MVA pathways for IPP biosynthesis, as well as for enzymes of the CP of amino acid biosynthesis (Figure 1), were defined as the best reciprocal hits resulting from all-against-all local BLASTP-searches with an E-value cutoff of 1E-5 and a bit score cutoff of 50 [52] using selected previously characterized sequences as queries (Additional file 6: Table S2). Only hits corresponding to full-length sequences were considered. Resulting hits were scanned for the presence of INTERPRO domains.

Phylogenetic analysis was performed on the basis of an alignment of protein sequences obtained using MUSCLE [53]. Maximum Likelihood (ML) phylogenetic reconstruction was carried out in PhyML v3.0 [54] using the LG protein evolution model [55] and heterogeneity of amino acid substitution rates corrected using a γ -distribution (G) with eight categories plus a proportion of invariant sites (I), selected by ProtTest v2.4 as the best-fitting amino acid substitution model according to the Akaike information criterion [56]. Starting phylogenetic trees were constructed using the modified program BIONJ. Tree topology searching was optimized using the subtree pruning and regrafting option. The statistical support of the retrieved topology was assessed using the Shimodaira-Hasegawa-like approximate likelihood ratio test (aLRT) [57].

Bayesian analysis was conducted in MrBayes v3.1.2 [58] using the WAG model [59] plus G with eight categories plus I. Searches were run using four Markov (MCMC) chains of length 1000000 generations sampling every 100th tree. Once stationary phase was reached (determined by the average standard deviation of split sequences approaching 0, which reflects convergence of independent tree samples), the first 2500 trees were discarded as burn-in, and a 50% majority-rule consensus tree was then constructed to evaluate Bayesian posterior probabilities on clades. Neighbor Joining phylogenetic analysis was performed in MEGA 5.0 [60]. The evolutionary distances for Neighbor Joining phylogenetic reconstruction were computed using the Poisson correction method. To obtain statistical support on the resulting clades, a bootstrap analysis with 1000 replicates was performed. Resulting trees were represented and edited using FigTree v1.3.1.

Analysis of functional divergence

The analysis of functional divergence was performed using DIVERGE v2.0 [61]. DIVERGE performs the ML estimation of the theta (θ) type-I and type-II coefficients of functional divergence, based on the occurrence of altered selective constraints or radical shifts of physicochemical properties, respectively [27,28]. θ value indicates the extent of functional divergence, ranging from 0, no functional divergence to 1, representing maximum divergence. Functional divergence can be explicitly tested by comparing the fit of a model allowing for functional divergence versus a null model in which functional divergence is not permitted ($\theta = 0$). A Likelihood Ratio Test (LRT) is then used to examine the significance of differences between the lnL values of the two nested models (calculated as $2\Delta\ln L$ -twice the difference between their lnL values) [62]. As the LRT asymptotically follows a χ^2 distribution with a number of degrees of freedom equal to one, i.e. the differences in number of parameters between the models being compared (θ), a p-value for the fitting of the model accounting for functional divergence can be computed. DIVERGE also uses a site-specific profile to estimate the posterior probabilities (Q_i) of individual amino acid sites to be critical for functional divergence.

G + C% content, dinucleotide frequencies, codon usage, and CAI analyses

The following sequence features i) GC% content at three codon positions and total (GC1, GC2, GC3 and GCt), ii) dinucleotide frequencies at 3:1 codon sites (third base and first base of the succeeding codon) and iii) the relative synonymous codon usages (RSCU) were extracted for individual DXR-II sequences and the rest of genes in the corresponding genomes through PERL and R scripts using cpan and bioperl modules. Codon Adaptation Indexes (CAI) [63] for individual genes and genomes were calculated using the method depicted in [64] as implemented in DAMBE software [65]. Comparative analyses of these sequence features between DXR-II genes and the rest of genes in the genome were performed and differences assessed using different statistical tests.

i) Differences in G and C nucleotides content were considered as significant when GC% deviated by two or more standard errors (SEs) regarding the respective means for all genes in the genome or deviations at first and third codon position were of the same sign and at least one was higher two or more SEs [35,66].

ii) Dinucleotide relative frequencies were calculated as:

$$\rho_{XY}^* = \frac{f_{XY}}{f_X f_Y}$$

Where f_X denotes the frequency of the mononucleotide X and f_{XY} the frequency of the dinucleotide XY. The

array of ρ_{XY} dinucleotide values define the genomic signature of a given species' genome [36]. A simple way to compute differences in dinucleotide relative frequencies between a given gene (f) and the value of the entire genome (g) is through the absolute difference (σ difference) calculated as:

$$\sigma^*(f, g) = \frac{1}{16} \sum_{XY} |\rho_{XY}^*(a) - \rho_{XY}^*(b)|$$

averaged over all 16 dinucleotides [67]. Furthermore, pairwise covariation of the 3:1 dinucleotide differences were assessed using the Spearman's rank correlation coefficient ρ [68] and the Kendall's rank correlation coefficient τ [69]. Both are nonparametric statistics allowing testing for dependence between two variables.

iii) RSCU provides with a simple effective measure of synonymous codon usage bias, in which codon frequencies are normalized by the frequency expected under the assumption of equal usage of synonymous codons for a given amino acid [70].

$$RSCU_i = \frac{X_i}{\frac{1}{n} \sum_{i=1}^n X_i}$$

For synonymous codon i of an n-fold degenerate amino acid, where X is the number of occurrences of codon i, and n the number of synonymous codons encoding for a given amino acid i.e. 1, 2, 3, 4, or 6. In the absence of any codon usage bias (i.e. all synonymous codons are used equally), the RSCU value would be 1. A codon that is used less or more frequently than expected will have an RSCU value < or > than 1, respectively. Start, stop and tryptophan codons were excluded from the analysis. To measure bias in synonymous codon usage between DXR-II and all genes in the genome, a χ^2 test of RSCU with 41 degrees of freedom was implemented [34].

iv) CAI was used as an alternative method to determine the degree of bias in the synonymous codon usage of the DXR-II gene regarding the optimal codon usage in the genome [34,63]. RSCU was firstly determined for all genes in each species genome, and subsequently used as reference set for the frequencies of the optimal codons in each species [65]. CAI is calculated as

$$CAI = \frac{CAI_{obs}}{CAI_{max}}$$

where CAI_{obs} is the mean of the RSCUs for all codons in a particular gene, and CAI_{max} is the mean of the RSCU for the most frequently used codons for an amino acid in a genome. CAI ranges from 0 to 1, being 1 if the gene only uses the most frequently used synonymous codons in the reference set. Differences in CAI between

DXR-II and all genes in the genome were considered as significant if higher than 1.5 times the SE.

Availability of supporting data

The multiple sequence alignment and the phylogenetic tree-files supporting the results of this article have been deposited and are publicly available in the TreeBASE repository under accession numbers: S14611 (<http://purl.org/phylo/treebase/phylows/study/TB2:S14611>).

Additional files

Additional file 1: Multiple alignment of 130 DRL and DLO related protein sequences. Positions conserved in 100%, 70% or 40% of the sequences are shown in black, dark grey and light grey, respectively. Strain names are grouped as DXR-II, DLO1 (grey shadow) and DLO2.

Additional file 2: ML phylogeny of DXR-II and DLO related sequences. ML cladogram depicting the evolutionary relationships among 53 DXR-II and 77 related protein sequences. Statistical support for clades (ML aLRT support values) is indicated next to nodes.

Additional file 3: Bayesian phylogeny of DXR-II and DLO related sequences. Bayesian cladogram depicting the evolutionary relationships among 53 DXR-II and 77 related protein sequences. Statistical support for clades (posterior probabilities) is indicated next to nodes.

Additional file 4: Neighbor Joining phylogeny of DXR-II and DLO related sequences. Neighbor Joining cladogram depicting the evolutionary relationships among 53 DXR-II and 77 related protein sequences. Statistical support for clades (bootstrap values) is indicated next to nodes.

Additional file 5: Complementation of DXR-deficient *E. coli* cells with putative DXR-II sequences from *Chloroflexus auranticus* J-10-fl. The putative DXR-II sequences were PCR-amplified from genomic DNA and cloned into pJET1.2. The corresponding constructs and positive and negative controls (C-, empty vector; C+, DXR-II (YP_418479.1) from *B. melitensis* biovar *abortus* 2308) were used to transform EcAB4-10 cells [23]. Ability of the cloned gene to rescue growth of this DXR-deficient mutant strain was ascertained by monitoring growth on plates either supplemented (+) or not (-) with 1 mM MVA as indicated. 1) YP_001634831.1, 2) YP_001634944.1, and 3) YP_001636771.1.

Additional file 6: Table S1. List of amino acid sites detected as related to functional divergence of DXR-II vs DLO1 and DXR-II vs DLO2.

Table S2. List of sequences used as queries in BLAST searches for enzymes of the MEP, MVA and CP pathway, and the corresponding bacterial strain. **Table S3.** Distribution of enzymes of the MEP, MVA and the CP pathways across 128 whole sequenced bacterial strains. **Table S4.** GC content of *DXR-II* genes and corresponding genomes. **Table S5.** 3:1 relative dinucleotide frequencies at *DXR-II* genes and their corresponding genomes and statistical tests of co-variation. **Table S6.** RSCU values at *DXR-II* genes and their corresponding genomes and statistical tests of independence. **Table S7.** CAI values for *DXR-II* genes and the average for all genes in the corresponding genomes.

Additional file 7: Distribution of DXR-I and DXR-II in Alphaproteobacteria. The occurrence of DXR-I and DXR-II is represented for alphaproteobacterial strains with full sequenced genomes in a phylogenetic context, according to the robust species tree reported in [30].

Additional file 8: Distribution of DXR-I and DXR-II in Firmicutes. The occurrence of DXR-I and DXR-II is represented for strains with full sequenced genomes in a phylogenetic context, according to the robust species tree for Firmicutes reported in [32].

Abbreviations

AK: Aspartokinase; ASDH: Aspartate semialdehyde dehydrogenase; CAI: Codon adaptation index; CP: Common pathway; HGT: Horizontal gene transfer; DLO: DXR-II-Like oxidoreductases; DXR: DeoxyXylulose 5-phosphate

reductoisomerase; DMAPP: DiMethylAllyl diphosphate; DXR like: DXR-II; HD: Homoserine dehydrogenase; HMGR: Hydroxy-3-Methyl-Glutaryl-CoA Reductase; IDI: IPP isomerase; IPP: Isopentenyl diphosphate; LRT: Likelihood ratio test; MEP: methylerythritol 4-phosphate; MVA: Mevalonate; ML: Maximum likelihood; RSCU: Relative synonymous codon usage; UID: (taxonomy) Unique Identifier.

Competing interests

The authors declare that they have no competing interests.

Authors' contributions

LCP and AL collected data. LCP, AL and JPG analysed data. LCP, AL, JPG, FJS, VAA and MRC contributed to the interpretation of the data. LCP and MRC conceived the study and participated in its design. LCP wrote the manuscript with significant contributions by JPG, FJS, VA and MRC. All authors have read and approved the final manuscript.

Acknowledgements

We thank all our laboratory members for stimulating discussions and suggestions. We thank Derek Taylor and Mario A Fares for critical reading of the manuscript and helpful comments. Financial support for this research was provided by the Spanish Ministerio de Ciencia e Innovación (grants BIO2011-23680 to MRC and BFU2011-25658 to FJS) and Generalitat de Catalunya (2009SGR-26 and XRB) to MRC.

Author details

¹Institute for Plant Molecular and Cell Biology - IBMCP (CSIC-UPV), Integrative Systems Biology Group, C/ Ingeniero Fausto Elio s/n., Valencia 46022, Spain. ²Department of Biological Sciences, SUNY-University at Buffalo, North Campus. 109 Cooke Hall, Buffalo, NY 14260, USA. ³Centre for Research in Agricultural Genomics (CRAG), CSIC-IRTA-UAB-UB, Campus UAB, Bellaterra, Barcelona 08193, Spain. ⁴Department of Molecular Biology, Universidad de Cantabria and Instituto de Biomedicina y Biotecnología de Cantabria (IBBTec), UC-CSIC-SODERCAN, Avda. de los Castros s/n, Santander E-39005Cantabria, Spain.

Received: 14 May 2013 Accepted: 16 August 2013

Published: 3 September 2013

References

1. Croteau R, Kutchan TM, Lewis NG: **Secondary Metabolites.** In *Biochemistry & Molecular Biology of Plants*. Edited by Buchanan WG B, Jones R, American Society of Plant Physiologists; 2000:1250-1318.
2. Daum M, Herrmann S, Wilkinson B, Bechthold A: **Genes and enzymes involved in bacterial isoprenoid biosynthesis.** *Curr Opin Chem Biol* 2009, **13**(2):180-188.
3. Kuzuyama T, Seto H: **Diversity of the biosynthesis of the isoprene units.** *Nat Prod Rep* 2003, **20**(2):171-183.
4. Rodríguez-Concepción M, Boronat A: **Elucidation of the methylerythritol phosphate pathway for isoprenoid biosynthesis in bacteria and plastids. A metabolic milestone achieved through genomics.** *Plant Physiol* 2002, **130**:1079-1089.
5. Lange BM, Rujan T, Martin W, Croteau R: **Isoprenoid biosynthesis: the evolution of two ancient and distinct pathways across genomes.** *Proc Natl Acad Sci U S A* 2000, **97**(24):13172-13177.
6. Begley M, Gahan CG, Kollas AK, Hintz M, Hill C, Jomaa H, Eberl M: **The interplay between classical and alternative isoprenoid biosynthesis controls gamma delta T cell bioactivity of *Listeria monocytogenes*.** *FEBS Lett* 2004, **561**(1-3):99-104.
7. Laupitz R, Hecht S, Amslinger S, Zepeck F, Kaiser J, Richter G, Schramek N, Steinbacher S, Huber R, Arigoni D, et al: **Biochemical characterization of *Bacillus subtilis* type II isopentenyl diphosphate isomerase, and phylogenetic distribution of isoprenoid biosynthesis pathways.** *Eur J Biochem* 2004, **271**(13):2658-2669.
8. Boucher Y, Doolittle WF: **The role of lateral gene transfer in the evolution of isoprenoid biosynthesis pathways.** *Mol Microbiol* 2000, **37**:703-716.
9. Phillips MA, Leon P, Boronat A, Rodríguez-Concepción M: **The plastidial MEP pathway: unified nomenclature and resources.** *Trends Plant Sci* 2008, **13**(12):619-623.
10. Jomaa H, Wiesner J, Sanderbrand S, Altincicek B, Weidemeyer C, Hintz M, Turbachova I, Eberl M, Zeidler J, Lichtenthaler HK, et al: **Inhibitors of the**

- nonmevalonate pathway of isoprenoid biosynthesis as antimalarial drugs. *Science* 1999, **285**(5433):1573–1576.
11. Kuzuyama T, Seto H: Two distinct pathways for essential metabolic precursors for isoprenoid biosynthesis. *Proc Jpn Acad Ser B Phys Biol Sci* 2012, **88**(3):41–52.
 12. Lichtenthaler HK: The 1-Deoxy-D-Xylulose-5-Phosphate pathway of Isoprenoid Biosynthesis in plants. *Annu Rev Plant Physiol Plant Mol Biol* 1999, **50**:47–65.
 13. Rodríguez-Concepción M, Boronat A: Isoprenoid biosynthesis in prokaryotic organisms. In *Isoprenoid Synthesis in Plants and Microorganisms*. Edited by Bach TJ, Rohmer M. New York: Springer; 2013:1–16.
 14. Rodríguez-Concepción M: The MEP pathway: a new target for the development of herbicides, antibiotics and antimalarial drugs. *Curr Pharm Des* 2004, **10**(19):2391–2400.
 15. Rohdich F, Bacher A, Eisenreich W: Isoprenoid biosynthetic pathways as anti-infective drug targets. *Biochem Soc Trans* 2005, **33**(Pt 4):785–791.
 16. Bouvier F, Rahier A, Camara B: Biogenesis, molecular regulation and function of plant isoprenoids. *Prog Lipid Res* 2005, **44**(6):357–429.
 17. Perez-Gil J, Rodríguez-Concepción M: Metabolic plasticity for isoprenoid biosynthesis in bacteria. *Biochem J* 2013, **452**(1):19–25.
 18. Boucher Y, Huber H, L'Haridon S, Stetter KO, Doolittle WF: Bacterial origin for the isoprenoid biosynthesis enzyme HMG-CoA reductase of the archaeal orders thermoplasmatales and archaeoglobales. *Mol Biol Evol* 2001, **18**(7):1378–1388.
 19. Gophna U, Thompson JR, Boucher Y, Doolittle WF: Complex histories of genes encoding 3-hydroxy-3-methylglutaryl-Coenzyme A reductase. *Mol Biol Evol* 2006, **23**(1):168–178.
 20. Kaneda K, Kuzuyama T, Takagi M, Hayakawa Y, Seto H: An unusual isopentenyl diphosphate isomerase found in the mevalonate pathway gene cluster from *Streptomyces* sp. strain CL190. *Proc Natl Acad Sci USA* 2001, **98**(3):932–937.
 21. Barkley SJ, Cornish RM, Poulter CD: Identification of an Archaeal type II isopentenyl diphosphate isomerase in methanothermobacter thermautotrophicus. *J Bacteriol* 2004, **186**(6):1811–1817.
 22. Barkley SJ, Desai SB, Poulter CD: Type II isopentenyl diphosphate isomerase from *Synechocystis* sp. strain PCC 6803. *J Bacteriol* 2004, **186**(23):8156–8158.
 23. Sangari FJ, Perez-Gil J, Carretero-Paulet L, Garcia-Lobo JM, Rodríguez-Concepción M: A new family of enzymes catalyzing the first committed step of the methylerythritol 4-phosphate (MEP) pathway for isoprenoid biosynthesis in bacteria. *Proc Natl Acad Sci U S A* 2010, **107**(32):14081–14086.
 24. Boucher Y, Douady CJ, Papke RT, Walsh DA, Boudreau MER, Nesbø CL, Case RJ, Doolittle WF: Lateral gene transfer and the origins of prokaryotic groups. *Annu Rev Genet* 2003, **37**:283–328.
 25. Moreno-Hagelsieb G, Latimer K: Choosing BLAST options for better detection of orthologs as reciprocal best hits. *Bioinformatics* 2008, **24**(3):319–324.
 26. Perez-Gil J, Calisto BM, Behrendt C, Kurz T, Fita I, Rodríguez-Concepción M: Crystal structure of brucella abortus deoxyxylulose-5-phosphate reductoisomerase-like (DRL) enzyme involved in isoprenoid biosynthesis. *J Biol Chem* 2012, **287**(19):15803–15809.
 27. Gu X: Statistical methods for testing functional divergence after gene duplication. *Mol Biol Evol* 1999, **16**(12):1664–1674.
 28. Gu X: A simple statistical method for estimating type-II (cluster-specific) functional divergence of protein sequences. *Mol Biol Evol* 2006, **23**(10):1937–1945.
 29. Humphrey W, Dalke A, Schulten K: VMD: visual molecular dynamics. *J Mol Graph* 1996, **14**(1):33–38. 27–38.
 30. Williams KP, Sobral BW, Dickerman AW: A robust species tree for the alphaproteobacteria. *J Bacteriol* 2007, **189**(13):4578–4586.
 31. Larimer FW, Chain P, Hauser L, Lamerdin J, Malfatti S, Do L, Land ML, Pelletier DA, Beatty JT, Lang AS, et al: Complete genome sequence of the metabolically versatile photosynthetic bacterium *Rhodospirillum rubrum*. *Nat Biotechnol* 2004, **22**(1):55–61.
 32. Moreno-Letelier A, Olmedo G, Eguarte LE, Martínez-Castilla L, Souza V: Parallel evolution and horizontal gene transfer of the *pst* operon in firmicutes from oligotrophic environments. *Int J Evol Biol* 2011, **2011**:781642.
 33. Fondi M, Brilli M, Fani R: On the origin and evolution of biosynthetic pathways: integrating microarray data with structure and organization of the common pathway genes. *BMC Bioinformatics* 2007, **8**(Suppl 1):S12.
 34. Lawrence JG, Ochman H: Amelioration of bacterial genomes: rates of change and exchange. *J Mol Evol* 1997, **44**(4):383–397.
 35. Lawrence JG, Ochman H: Molecular archaeology of the *Escherichia coli* genome. *Proc Natl Acad Sci U S A* 1998, **95**(16):9413–9417.
 36. Karlin S, Burge C: Dinucleotide relative abundance extremes: a genomic signature. *Trends Genet* 1995, **11**(7):283–290.
 37. Hooper SD, Berg OG: Detection of genes with atypical nucleotide sequence in microbial genomes. *J Mol Evol* 2002, **54**(3):365–375.
 38. Genschel U: Coenzyme A biosynthesis: reconstruction of the pathway in archaea and an evolutionary scenario based on comparative genomics. *Mol Biol Evol* 2004, **21**(7):1242–1251.
 39. Gherardini PF, Wass MN, Helmer-Citterich M, Sternberg MJ: Convergent evolution of enzyme active sites is not a rare phenomenon. *J Mol Biol* 2007, **372**(3):817–845.
 40. Kulkarni N, Lakshmikumar M, Rao M: Xylanase II from an alkaliphilic thermophilic *Bacillus* with a distinctly different structure from other xylanases: evolutionary relationship to alkaliphilic xylanases. *Biochem Biophys Res Commun* 1999, **263**(3):640–645.
 41. Watanabe S, Yamada M, Ohtsu I, Makino K: alpha-ketoglutaric semialdehyde dehydrogenase isozymes involved in metabolic pathways of D-glucarate, D-galactarate, and hydroxy-L-proline. Molecular and metabolic convergent evolution. *J Biol Chem* 2007, **282**(9):6685–6695.
 42. Brocks JJ, Logan GA, Buick R, Summons RE: Archean molecular fossils and the early rise of eukaryotes. *Science* 1999, **285**(5430):1033–1036.
 43. Iguchi E, Okuhara M, Kohsaka M, Aoki H, Imanaka H: Studies on new phosphonic acid antibiotics. II. Taxonomic studies on producing organisms of the phosphonic acid and related compounds. *J Antibiot (Tokyo)* 1980, **33**(1):19–23.
 44. Guptill L: Bartonellosis. *Vet Microbiol* 2010, **140**(3–4):347–359.
 45. Allerberger F, Wagner M: Listeriosis: a resurgent foodborne infection. *Clin Microbiol Infect* 2010, **16**(1):16–23.
 46. von Bargen K, Gorvel JP, Salcedo SP: Internal affairs: investigating the brucella intracellular lifestyle. *FEMS Microbiol Rev* 2012, **36**(3):533–562.
 47. Wells CL, Wilkins TD: Clostridia: sporeforming anaerobic bacilli. In *Medical Microbiology*. 4th edition. Edited by Baron S. Galveston (TX); 1996.
 48. Ochman H, Lawrence JG, Groisman EA: Lateral gene transfer and the nature of bacterial innovation. *Nature* 2000, **405**(6784):299–304.
 49. Kunin V, Ouzounis CA: The balance of driving forces during genome evolution in prokaryotes. *Genome Res* 2003, **13**(7):1589–1594.
 50. Kurland CG, Canback B, Berg OG: Horizontal gene transfer: a critical view. *Proc Natl Acad Sci U S A* 2003, **100**(17):9658–9662.
 51. Mirkin BG, Fennner TI, Galperin MY, Alparone EV: Algorithms for computing parsimonious evolutionary scenarios for genome evolution, the last universal common ancestor and dominance of horizontal gene transfer in the evolution of prokaryotes. *BMC Evol Biol* 2003, **3**:2.
 52. Altschul SF, Madden TL, Schaffer AA, Zhang J, Zhang Z, Miller W, Lipman DJ: Gapped BLAST and PSI-BLAST: a new generation of protein database search programs. *Nucleic Acids Res* 1997, **25**(17):3389–3402.
 53. Edgar RC: MUSCLE: multiple sequence alignment with high accuracy and high throughput. *Nucleic Acids Res* 2004, **32**(5):1792–1797.
 54. Guindon S, Dufayard JF, Lefort V, Anisimova M, Hordijk W, Gascuel O: New algorithms and methods to estimate maximum-likelihood phylogenies: assessing the performance of PhyML 3.0. *Syst Biol* 2010, **59**(3):307–321.
 55. Le SQ, Gascuel O: An improved general amino acid replacement matrix. *Mol Biol Evol* 2008, **25**(7):1307–1320.
 56. Abascal F, Zardoya R, Posada D: ProtTest: selection of best-fit models of protein evolution. *Bioinformatics* 2005, **21**(9):2104–2105.
 57. Anisimova M, Gascuel O: Approximate likelihood-ratio test for branches: a fast, accurate, and powerful alternative. *Syst Biol* 2006, **55**(4):539–552.
 58. Ronquist F, Huelsenbeck JP: MrBayes 3: Bayesian phylogenetic inference under mixed models. *Bioinformatics* 2003, **19**(12):1572–1574.
 59. Whelan S, Goldman N: A general empirical model of protein evolution derived from multiple protein families using a maximum-likelihood approach. *Mol Biol Evol* 2001, **18**(5):691–699.
 60. Tamura K, Dudley J, Nei M, Kumar S: MEGA4: Molecular Evolutionary Genetics Analysis (MEGA) Software Version 4.0. *Mol Biol Evol* 2007, **24**(8):1596–1599.
 61. Gu X, Vander Velden K: DIVERGE: phylogeny-based analysis for functional-structural divergence of a protein family. *Bioinformatics* 2002, **18**(3):500–501.
 62. Goldman N, Yang Z: A codon-based model of nucleotide substitution for protein-coding DNA sequences. *Mol Biol Evol* 1994, **11**(5):725–736.

63. Sharp PM, Li WH: The codon Adaptation Index—a measure of directional synonymous codon usage bias, and its potential applications. *Nucleic Acids Res* 1987, **15**(3):1281–1295.
64. Xia X: An improved implementation of codon adaptation index. *Evol Bioinform Online* 2007, **3**:53–58.
65. Xia X, Xie Z: DAMBE: software package for data analysis in molecular biology and evolution. *J Hered* 2001, **92**(4):371–373.
66. Garcia-Vallve S, Romeu A, Palau J: Horizontal gene transfer in bacterial and archaeal complete genomes. *Genome Res* 2000, **10**(11):1719–1725.
67. Karlin S: Detecting anomalous gene clusters and pathogenicity islands in diverse bacterial genomes. *Trends Microbiol* 2001, **9**(7):335–343.
68. Spearman C: The proof and measurement of association between Two things. *Am J Psychol* 1904, **15**(1):72–101.
69. Kendall MG: A new measure of rank correlation. *Biometrika* 1938, **30**(1–2):81–93.
70. Sharp PM, Tuohy TM, Mosurski KR: Codon usage in yeast: cluster analysis clearly differentiates highly and lowly expressed genes. *Nucleic Acids Res* 1986, **14**(13):5125–5143.

doi:10.1186/1471-2148-13-180

Cite this article as: Carretero-Paulet *et al.*: Evolutionary diversification and characterization of the eubacterial gene family encoding DXR type II, an alternative isoprenoid biosynthetic enzyme. *BMC Evolutionary Biology* 2013 **13**:180.

Submit your next manuscript to BioMed Central and take full advantage of:

- Convenient online submission
- Thorough peer review
- No space constraints or color figure charges
- Immediate publication on acceptance
- Inclusion in PubMed, CAS, Scopus and Google Scholar
- Research which is freely available for redistribution

Submit your manuscript at
www.biomedcentral.com/submit

